frontiers | Frontiers in Earth Science

TYPE Original Research
PUBLISHED 26 October 2023
DOI 10.3389/feart.2023.1259831

OPEN ACCESS

EDITED BY
Fabio Luca Bonali,
University of Milano-Bicocca, Italy

REVIEWED BY
Andrea Zanchi,
University of Milano-Bicocca, Italy
Francesco Muto,
University of Calabria, Italy

*CORRESPONDENCE
A. Akimbekova,
asselakimbekova@gmail.com

RECEIVED 16 July 2023
ACCEPTED 05 October 2023
PUBLISHED 26 October 2023

CITATION
Akimbekova A, Carboni F, Mancinelli P, Barreca G, Scarfì L, Pauselli C, Monaco C and Barchi MR (2023), Gravity modelling of the Tyrrhenian-Calabrian-Ionian subduction system.
Front. Earth Sci. 11:1259831.
doi: 10.3389/feart.2023.1259831

Gravity modelling of the Tyrrhenian-Calabrian-Ionian subduction system

A. Akimbekova[1]*, F. Carboni[1], P. Mancinelli[2], G. Barreca[3], L. Scarfì[4], C. Pauselli[1], C. Monaco[3] and M. R. Barchi[1]

[1]Dipartimento di Fisica e Geologia, Università degli Studi di Perugia, Perugia, Italy, [2]Department of Engineering and Geology, G. d'Annunzio University of Chieti and Pescara, Pescara, Italy, [3]Dipartimento di Scienze Biologiche, Geologiche e Ambientali, Università di Catania, Catania, Sicily, Italy, [4]Istituto Nazionale di Geofisica e Vulcanologia, Osservatorio Etneo, Catania, Italy

This study provides a lithospheric-scale model along the Ionian Subduction zone in Southern Italy, contributing to the seismotectonic investigation of a region which is affected by relevant historical seismicity. The study employs gravity forward modelling to build the geo-structural model along a composite, NW-SE trending transect extending from the Ionian to the Tyrrhenian Sea, including the Aeolian arc and the Calabro-Peloritan onshore. Through a multidisciplinary approach, we propose new interpretations of three 2D deep-seismic reflection profiles across the study area. Such interpretative profiles are used as constraints to model the observed Bouguer gravity anomalies providing upper and lower crust geometries. Whilst a tomographic model provides constraints for the lithospheric and asthenospheric modelling. The entire workflow is constrained by literature data about Moho geometry, deep seismicity and tomographic images that are integrated to determine the subducting slab geometry. The proposed model of the entire subducting system reasonably fits the observed gravity field and is coherent with the first-order geological and geophysical constraints. The modelling results in updated Tyrrhenian and Ionian Moho depth, subducting slab geometry and location, and densities of the main units, providing valuable input about the composition and geometry of the Calabrian arc structures.

KEYWORDS

Calabrian Arc (Italy), subducion complex, gravity forward modeling, crustal model, Ionian Subduction zone, Tyrrhenian back-arc basin-calabrian arc-accretionary wedge system, Southern Italy

1 Introduction

The aim of this study is to reconstruct a geo-structural model of the crustal and sub-crustal structure of the Tyrrhenian- Calabrian-Ionian subduction system in Southern Italy (Scandone, 1979). Gravity forward modelling, along with the interpretation of available deep-penetrating seismic lines (i.e., CROP Project, Scrocca et al., 2003), have been used to build the geo-structural model along a transect extending from the Ionian to the Tyrrhenian Sea, including onshore Calabria (Figure 1).

The trace of the modelled transect (Figure 1) is composed of two segments with different orientations: the NW-SE trending, Eastern part follows the trace of the CROP M4 line in the Ionian off-shore. While the WNW-ESE trending, the Western part runs in-between the CROP M27 and the M2AA lines in the Tyrrhenian off-shore, extending eastward through the Calabria onshore. Starting from the NW, the proposed transect crosses the following

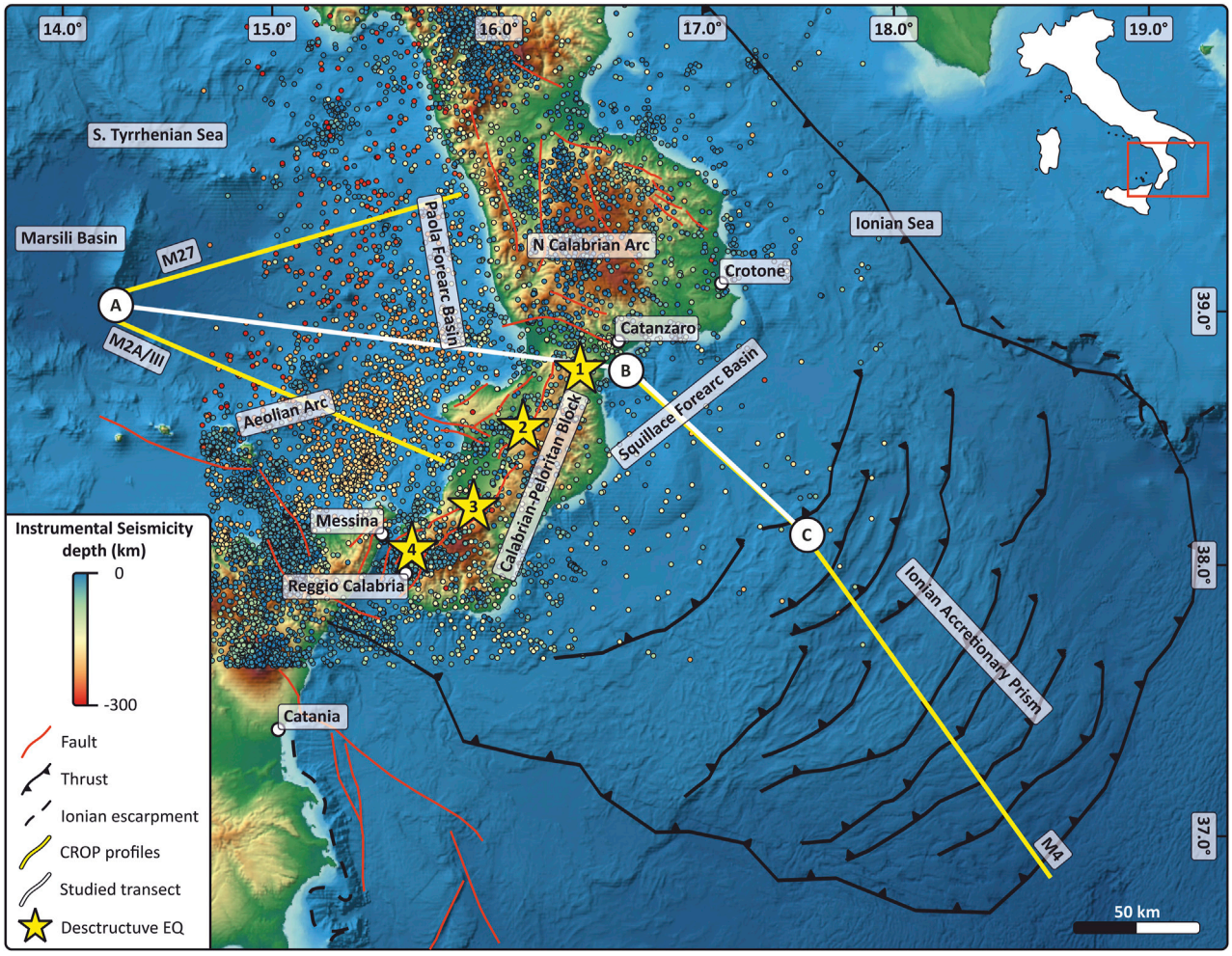

FIGURE 1
Geological map showing the main features within the study area, including: i) seismic reflection profiles, ii) modelled transect which corresponds to the length of the tomography, iii) instrumental seismicity, iii) the main tectonic features, iv) historical destructive seismicity (1. Mw 7.0, 2. Mw 6.7, 3. Mw 7.1, 4. Mw 7.1). Across the study area, the topography ranges between 0 and 828 m a. s. l., while bathymetry reaches 3445 m in the Tyrrhenian Sea and 2010 m in the Ionian Sea. Topography and bathymetry data are from the Global Relief Model (Gebco compilation group, 2020).

tectonic domains: the Tyrrhenian back-arc basin, the Aeolian volcanic arc, the Paola fore-arc basin, the onshore Southern Calabrian-Peloritan block, and the thick and wide accretionary wedge in the Ionian Sea, floored by the oldest (Permian-Triassic age) oceanic crust of the Mediterranean Sea (Finetti, 1982; De Voogd et al., 1992; Finetti et al., 1996; Stampfli et al., 1998; Catalano et al., 2001; Speranza et al., 2012; Dellong et al., 2018; Tugend et al., 2019).

This study is based on a multidisciplinary approach where 2D deep seismic reflection profiles, seismicity, and tomographic images are integrated to provide constraints for the modelling of the observed Bouguer gravity anomalies. In fact, if properly constrained, the forward or inverse modelling of the Bouguer gravity anomaly has proven reliable for the investigation at different scales since it is capable of unveiling crustal and sub-crustal structures (e.g., Tassis et al., 2013; Mancinelli et al., 2020; Akimbekova et al., 2021; Mancinelli et al., 2021). In particular, gravity anomalies at subduction zones are generally characterized by strong signatures that are linked to topographic effects, material density, and temperature heterogeneities in the lithospheric mantle and the crust or even forces and stresses induced by plate dynamics (e.g., Marotta et al., 2006; Bassett and Watts, 2015).

The Bouguer gravity anomaly data used in this work (Figure 2A) derive from the 1:500,000 Gravity map of Italy (C.N.R.-P.F.G., 1991), where data originally acquired by AGIP and CNR, consisting of ~270,000 station measurements, were gathered. The dataset was gridded through 1 km × 1 km spacing and 85,952 nodes. The Bouguer reduction was calculated using a density of 2,670 kg m^{-3}.

Along the modelled transect, anomaly maxima are located in the Tyrrhenian Sea at the north-western end of the transect, while the regional trend decreases towards the southeast, reaching a minimum of 20 mGal on the Ionian coastline of Calabria (Figure 2B). Gravity anomaly values gently increase in the south-eastern part of the modelled transect, towards the Ionian Abyssal Plain.

By exploring the subsurface setting of the Tyrrhenian-Calabrian-Ionian subduction system (TCISS hereinafter), this study is also aimed at providing contributions to the seismotectonic understanding of a region

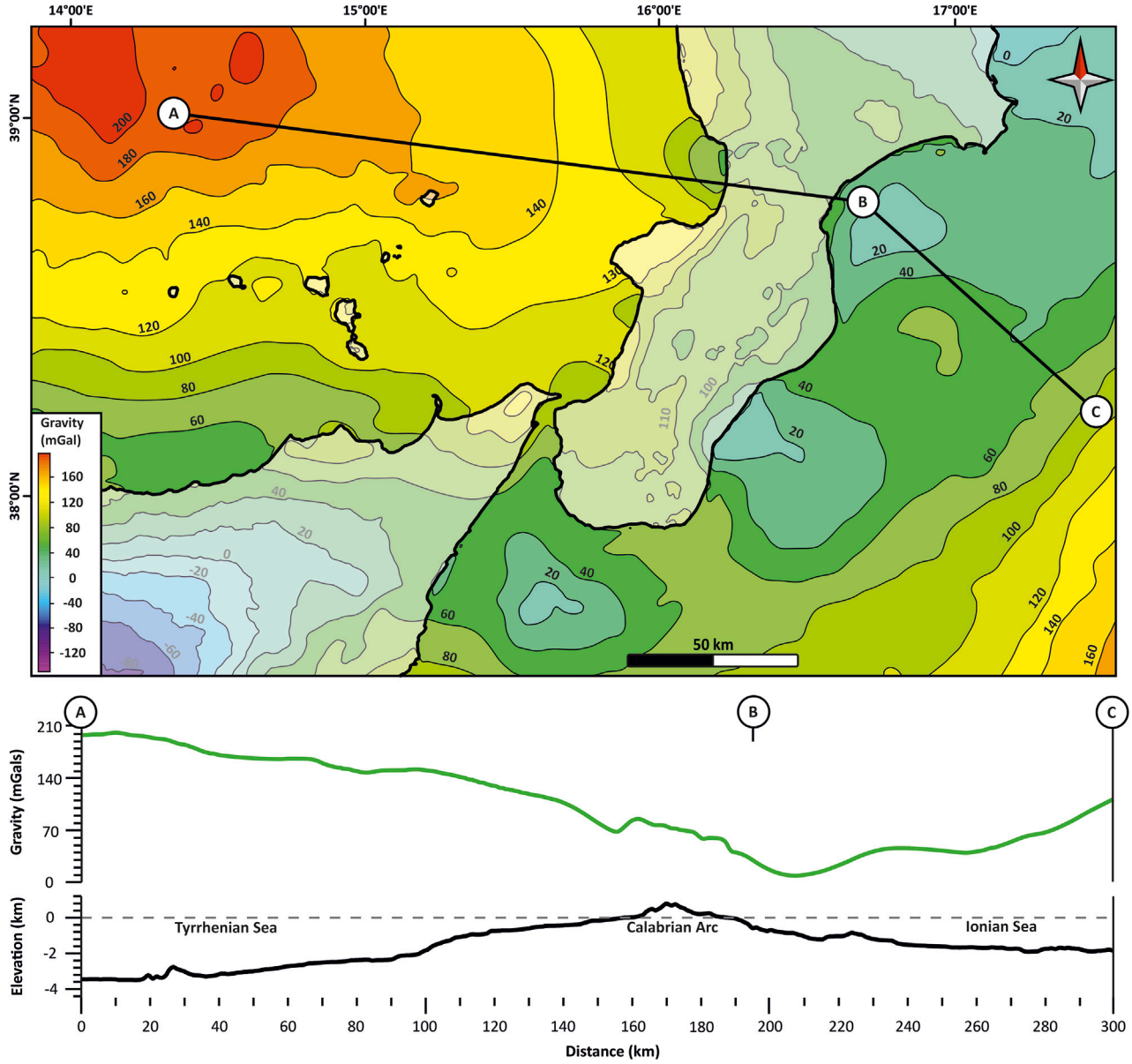

FIGURE 2
(A) Bouguer gravity anomaly map of across the study area. **(B)** Profile view of the observed Bouguer gravity (above) and of topography/bathymetry (below), along the modelled transect. Across the modelled profile, the topography ranges between 0 and 828 m a.s.l. on the Calabrian onshore, while bathymetry reaches −3500 m b.s.l. in the Marsili basin in the southern Tyrrhenian Sea and −2000 m in the Ionian Sea.

of Southern Italy, which is affected by relevant seismicity, including also some significant historical destructive seismic events (Figure 1), whose causative faults are still unknown or debated. Even though historical destructive earthquakes are associated with normal faulting in onshore Calabria (Monaco and Tortorici, 2000; Jacques et al., 2001), still the subduction interface is the source of deep earthquakes responsible for most of the moderate seismicity registered in the Calabrian Arc region. Thus, investigating the deep crustal structures, especially the location and geometry of the Ionian slab, may result useful to reveal what processes are causing the seismicity of the area. In particular, modelling the boundary between the downgoing slab and the upper plate along the subduction zone is crucial for assessing the potential of this subducting zone to generate megathrust earthquakes. However, such investigation would be impossible without geological and geophysical constraints about the lithosphere and the asthenosphere over the target area. Following a classical geophysical modeling approach, we search for those constraints in previous works and independent data. After a compelling review of the available literature about the geophysical investigation of the Ionian subduction, we provide an interpretative view of three depth-converted crustal-scale seismic reflection profiles cross-cutting the Tyrrhenian and Ionian Sea. The crustal geometries resulting from those seismic data, coupled with a tomographic model over the same area, provide the required constraints for the lithospheric scale forward modeling of the observed Bouguer gravity anomaly.

2 Geological and geodynamic setting

The Tyrrhenian-Calabrian-Ionian subduction system in the Central Mediterranean is the result of the Neogene-Quaternary subduction of the narrow Ionian slab below the Calabrian Arc and the Tyrrhenian basin (Scandone, 1979).

The Calabrian Arc (CA) in Southern Italy is an arc-shaped terrane (Malinverno and Ryan, 1986; Johnston and Mazzoli, 2009) of European-derived continental rocks surrounded by deep-water basins of different nature and age, the Pliocene-Pleistocene back-arc Tyrrhenian Sea to the West and the much older Ionian remnant of the Mesozoic Neo-Tethys (Sengör, 1979) to the East. The CA is mostly composed of the Variscan metamorphic basement and remnants of Mesozoic-Cenozoic carbonate and clastic covers (Ogniben, 1973; Amodio-Morelli et al., 1976).

Despite that subduction has slowed down starting from the Middle Pleistocene (Goes et al., 2004) and the slab has undergone detachment processes both longitudinally and transversally (Scarfì et al., 2018), the seismicity is distributed along a well-defined Wadati-Benioff zone with focal depth that is less than 50 km in the Ionian Basin and down to 660 km in the Tyrrhenian Basin (Selvaggi and Chiarabba, 1995; Engdahl et al., 1998). As regards the Ionian slab, recent studies based on wide-angle seismic survey imaged a 5- to 6-km-thick oceanic crust in the Ionian basin (Dellong et al., 2018; Dannowski et al., 2019). According to many authors (e.g., Catalano et al., 2001; Speranza et al., 2012), the opening of this diverging basin occurred since the Late Triassic to the Late Jurassic-Early Cretaceous along the northern margin of the African plate, between the Pelagian and the Apulian blocks. Other studies propose ages ranging between the Late Triassic and the Early Jurassic (Frizon de Lamotte et al., 2011; Gallais et al., 2011). Multichannel seismic studies show that sediments accumulated above the Ionian crust increase their thickness from about 5 km in the abyssal plain to 10–15 km within the accretionary wedge, with the subducting plate (dipping 1°–2° on average) steepening as it approaches the CA (Cernobori et al., 1996; Minelli and Faccenna, 2010; Gallais et al., 2011; Polonia et al., 2011; Maesano et al., 2017).

In the frame of the Neogene-Quaternary tectonic convergence between African and European plates, the CA and its continental roots form the upper plate of the Ionian Subduction Zone (ISZ), acting as a backstop of the accretionary wedge, whereas the Ionian oceanic lithosphere forms the lower plate. The Ionian basin represents an oceanic crustal compartment of the African plate, laterally confined by the WNW-ESE trending Apulia and Malta escarpments to its northern and southern boundaries, respectively (Scandone et al., 1981; Fabbri et al., 1982; Casero et al., 1984). This crustal setting is inherited from the Permian–Triassic rifting phase, followed by the subsequent Jurassic–Cretaceous spreading stage (Ben-Avraham and Grasso, 1991; Catalano et al., 2001). According to the original paleogeographic configuration, the laterally variable (continental to oceanic) African margin has been progressively involved in subduction (oceanic versus continental) and collision (continental versus continental) during the Neogene tectonic shortening (Scandone, 1979). In this frame, the denser Ionian oceanic lithosphere began to underplate toward the NW beneath Iberia and France, of which the Sardinia-Corsica and the Calabro-Peloritan continental blocks were parts (Jolivet and Faccenna, 2000). Since ~35 Ma, the rapid SE-wards rolling-back of the Ionian slab has controlled the tectonic evolution of the Western Mediterranean region, resulting in the opening of two large back-arc extensional basins, i.e., the older Ligurian-Provençal basin and the younger Tyrrhenian basin (Scandone, 1979; Malinverno and Ryan, 1986; Patacca and Scandone, 1989; Faccenna et al., 2004), combined with upper plate delamination and fragmentation (Ghisetti and Vezzani, 1982). The back-arc opening was accompanied by trench migration and by the consequent accretion of a set of imbricated, foreland-verging orogenic wedges (e.g., Faccenna et al., 2014 and references therein). In this setting, the SE-ward advancement of the Calabrian backstop toward the unconstrained Ionian basin resulted in the formation of an up to 150 km wide accretionary wedge in the Ionian Sea (Minelli and Faccenna, 2010).

The current tectonic setting in the upper plate of the ISZ is that of an intricate back-arc/fore-arc/trench system (Scandone, 1979; Malinverno and Ryan, 1986; Patacca and Scandone, 1989; Faccenna et al., 2004) where volcanism (De Astis et al., 2003), extensional faulting (Monaco and Tortorici, 2000), uplifting (Ferranti et al., 2006), frontal thrusting (Minelli and Faccenna, 2010; Polonia et al., 2011) and slab-edge tear deformation (Barreca et al., 2014; 2019; Gutscher et al., 2016; Polonia et al., 2016; Cultrera et al., 2017; Scarfì et al., 2018) have taken place simultaneously. The lower plate setting is imaged at depth by the occurrence of intermediate to deep seismicity beneath the Calabrian Arc (Latorre et al., 2023), where hypocenters well define a narrow descending slab with a Wadati-Benioff plane that is continuous down to 600 km depth (Frepoli et al., 1996), as well as by tomographic models of the lithosphere (e.g., Wortel and Spakman, 2000; Neri et al., 2012; Calò et al., 2012; Scarfì et al., 2018). Even though the near-cessation of the Calabrian roll-back and stalling of the slab subduction has been proposed (Faccenna et al., 2001; Goes et al., 2004), residual trench migration <5 mm/yr), see D'Agostino et al., 2008 & 2011) point to a still slowly receding slab.

3 Previous studies of the Moho and lithosphere

3.1 Ionian vs. Tyrrhenian Moho

Prior to starting the modelling along the transect, we performed a compelling review of the available literature about the Moho depth across the study area. We collected interpretations of data acquired through both active and passive seismic methods, like DSS, seismic refraction/reflection, teleseismic and gravity data (Scarascia et al., 1994; Nicolich, 2001; Finetti, 2005; Cassinis et al., 2003; Piana Agostinetti and Amato, 2009; Di Stefano et al., 2011; Mele, 2012). Data retrieved from the aforementioned works reveal some discrepancies between the proposed Moho geometries at depth (Figure 3). However, all interpretations highlight the occurrence of two distinct Moho surfaces, characterizing the NW and the SE part of the transect, respectively: a shallower, gently SE-dipping Tyrrhenian Moho beneath the Tyrrhenian Sea and a relatively deeper and steeper, NW-dipping Ionian Moho in the SE side of the profile. In the central part of the transect beneath the Calabrian onshore, the Tyrrhenian crust is tectonically superposed to the Ionian crust: the intersection between the two superposed Moho discontinuities localizes the plate boundary at depth.

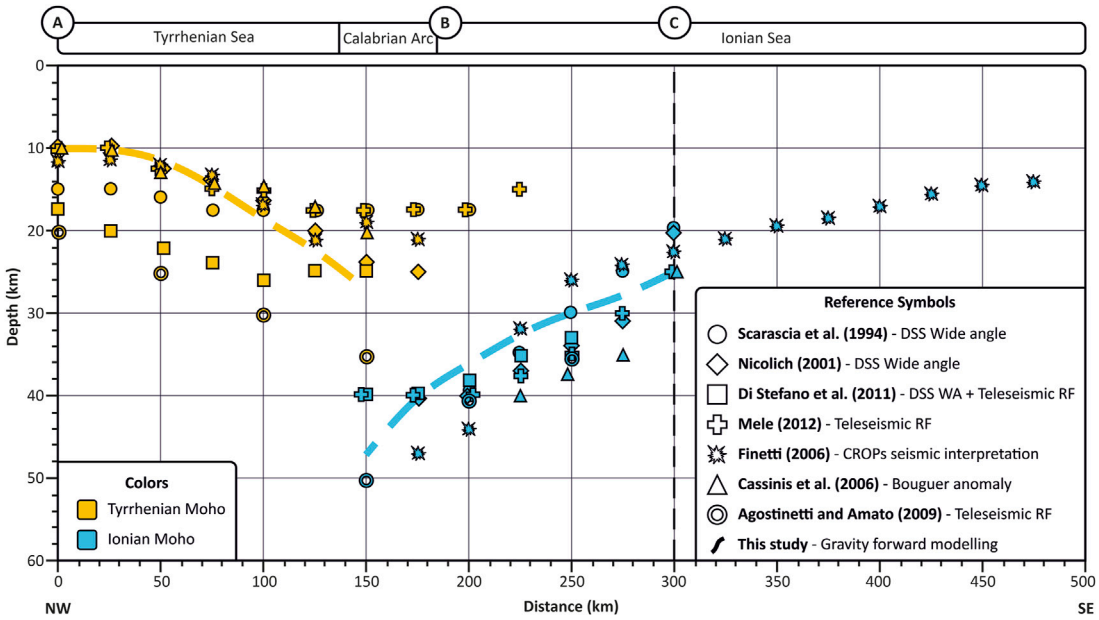

FIGURE 3
Moho depth interpretations along the modelled transect (see the trace in Figure 1), as proposed in the works listed in the legend box, together with the corresponding method.

The comparison between the different Moho interpretations shows that in the upper plate region (i.e., beneath the Tyrrhenian Sea, 0–150 km), the depth of the Tyrrhenian Moho ranges between 10 and 20 km according to all the aforementioned models. Moving towards the SE, the Tyrrhenian Moho gently deepens beneath the Calabria coastline down to a depth of 35 km (yellow data points in Figure 3). In the lower plate region (SE portion of the profile), the Ionian Moho depth ranges between 14 km in the Ionian offshore (Finetti, 2005) and 50 km by moving NW-ward along the modelled profile. According to previous studies (Scarascia et al., 1994; Nicolich, 2001; Finetti, 2005; Cassinis et al., 2003; Piana Agostinetti and Amato, 2009; Di Stefano et al., 2011; Mele, 2012) between km 300 and km 150, the Ionian Moho depth is more uncertain since it carries local discrepancies up to 13 km wide (blue data points in Figure 3). Considering all these data, for our model we adopted a geometry and depth of Moho discontinuity in agreement with observed Bouguer anomalies.

3.2 Lithosphere/upper asthenosphere structure

Along our profile, the models proposed by Pontevivo and Panza (2006), using nonlinear inversion of surface-wave data, locate a very shallow lithosphere/asthenosphere boundary at around 20 km of depth in the southern Tyrrhenian Basin (B4 cell in their work) and at 135 km depth in the south-eastern part of our profile corresponding to Ionian Sea (cell C7 in their work). Below the Calabria block, a serpentinized layer ranging between ~110 and 170 km depth is reported by the same authors (see cell C6).

4 Deep crustal seismic (CROP) profiles interpretation

Three deep seismic reflection profiles (traces on Figure 1), acquired in the framework of the CROP Project (Scrocca et al., 2003) were interpreted and depth-converted in the present study: two lines crossing the Southern Tyrrhenian Sea (lines M27 and M2AA) and one crossing the Ionian Sea, (line M4). The interpretation of the three deep seismic reflection profiles aims at constraining the major stratigraphic and structural features within the crust in order to provide reliable geometries for gravity modelling. A detailed seismo-stratigraphic interpretation of these CROP profiles has been provided by Finetti (2005).

Starting from the tectono-stratigraphic interpretation in TWT (clean lines - Figures 4A, 5A, 6A and interpreted lines—Figures 4B, 5B, 6B), the profiles were time-to-depth converted (Figures 4C, 5C, 6C) using average velocities, selected according to previously published velocity models, as summarised in Table 1 (e.g., Scarascia et al., 1994; Neri et al., 2009; Pepe et al., 2010; Polonia et al., 2011; Dellong et al., 2018; Scarfì et al., 2018).

4.1 M4 CROP profile

The NW-SE trending deep seismic profile M4 (Figure 4) has been acquired in the offshore SE of Calabria across the wide and thick Ionian accretionary wedge.

The profile mainly shows the tectono-stratigraphic structure and thickness of the Ionian accretionary wedge. The accretionary wedge is a well-visible feature that can be followed for about 250 km and up to 25 km of depth in its inner portion, made up of Mesozoic–Cenozoic sediments (Polonia et al., 2011), internally deformed by NW-dipping

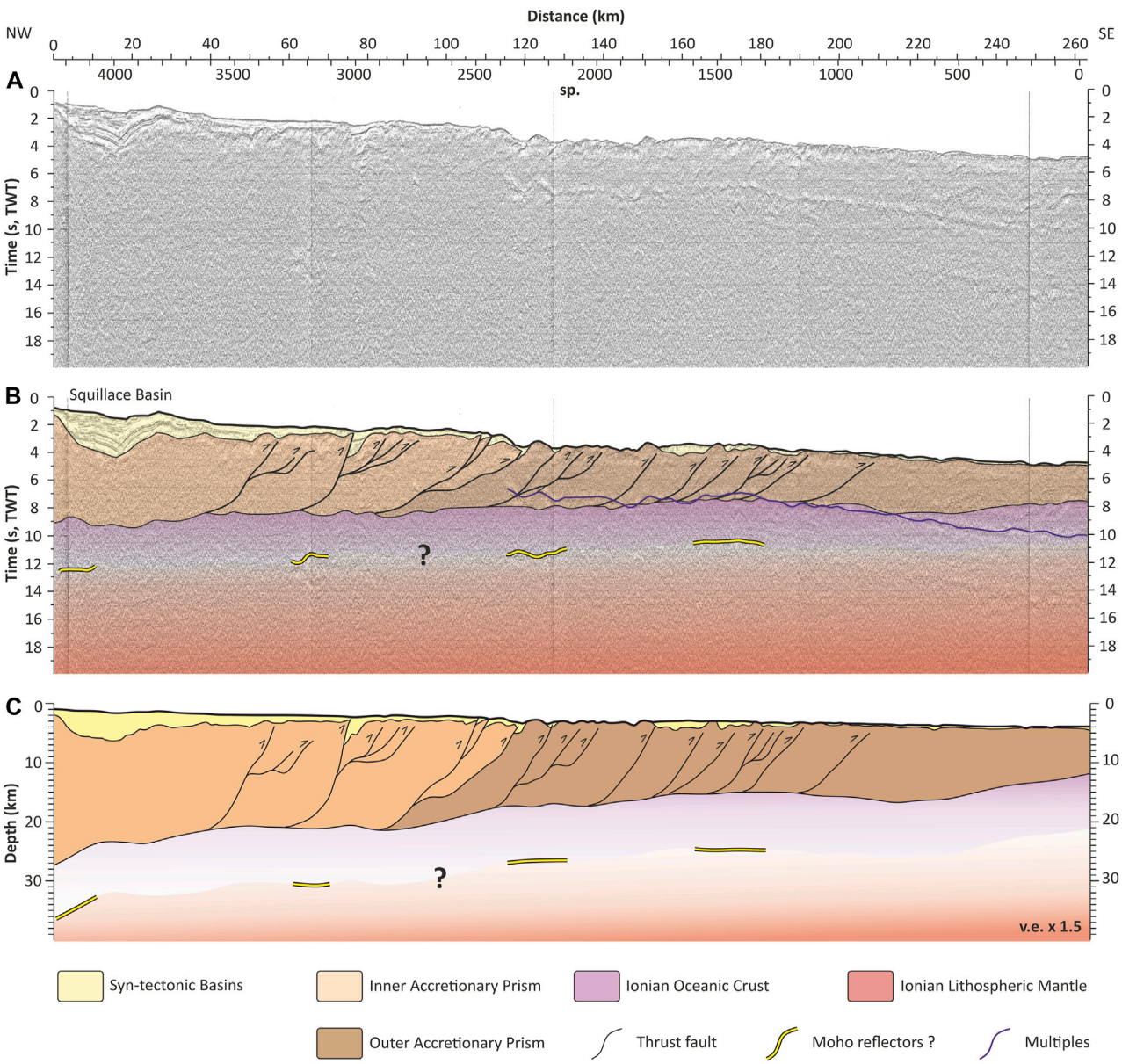

FIGURE 4
Interpreted M4 CROP NVR profile in time clean **(A)** and interpreted **(B)** and depth converted domains **(C)**.

imbricated thrusts has been described in a wide range of literature (e.g., Finetti, 2005; Minelli and Faccenna, 2010; Polonia et al., 2011; Gutscher et al., 2017; Maesano et al., 2017). Polonia et al. (2011) subdivided the wedge into two lobes: eastern and western. Our study transect is located in the eastern part, which is structurally split into Post-Messinian salt bearing (outer) and Pre-Messinian clastic (inner) accretionary wedge.

Additionally, a detailed interpretation provided by Finetti (2005) suggests the occurrence of two structural domains within the accretionary prism: an inner domain made up of shortened continental sediments and an eastern domain, consisting of imbricated slices made up of the obducted deep-water sediments covering the Mesozoic oceanic crust of the Ionian Sea.

The shallowest portion of the accretionary wedge hosts thrust-top basins infilled by recent, syn-tectonic sediments. The Squillace basin (between shot points 4,200–3,800, close to the Ionian Calabria coastline) is the most prominent syn-tectonic basin along the transect. It is characterized by well-stratified seismic facies bounded by several angular unconformities, indicating a complex interaction between tectonic and sedimentation. At the depocenter, the basin is filled by a thick (ca. 5 km) sequence of Neogene–Quaternary sediments, mainly composed of clastic sequences and Messinian salt (Minelli and Faccenna, 2010). The thickness of the syntectonic sediments decreases towards the SE, where they also appear less deformed.

The Top of the Ionian oceanic crust was traced following a strong set of reflectors between 7 and 9 s (TWT section at Figure 4), also imaged by

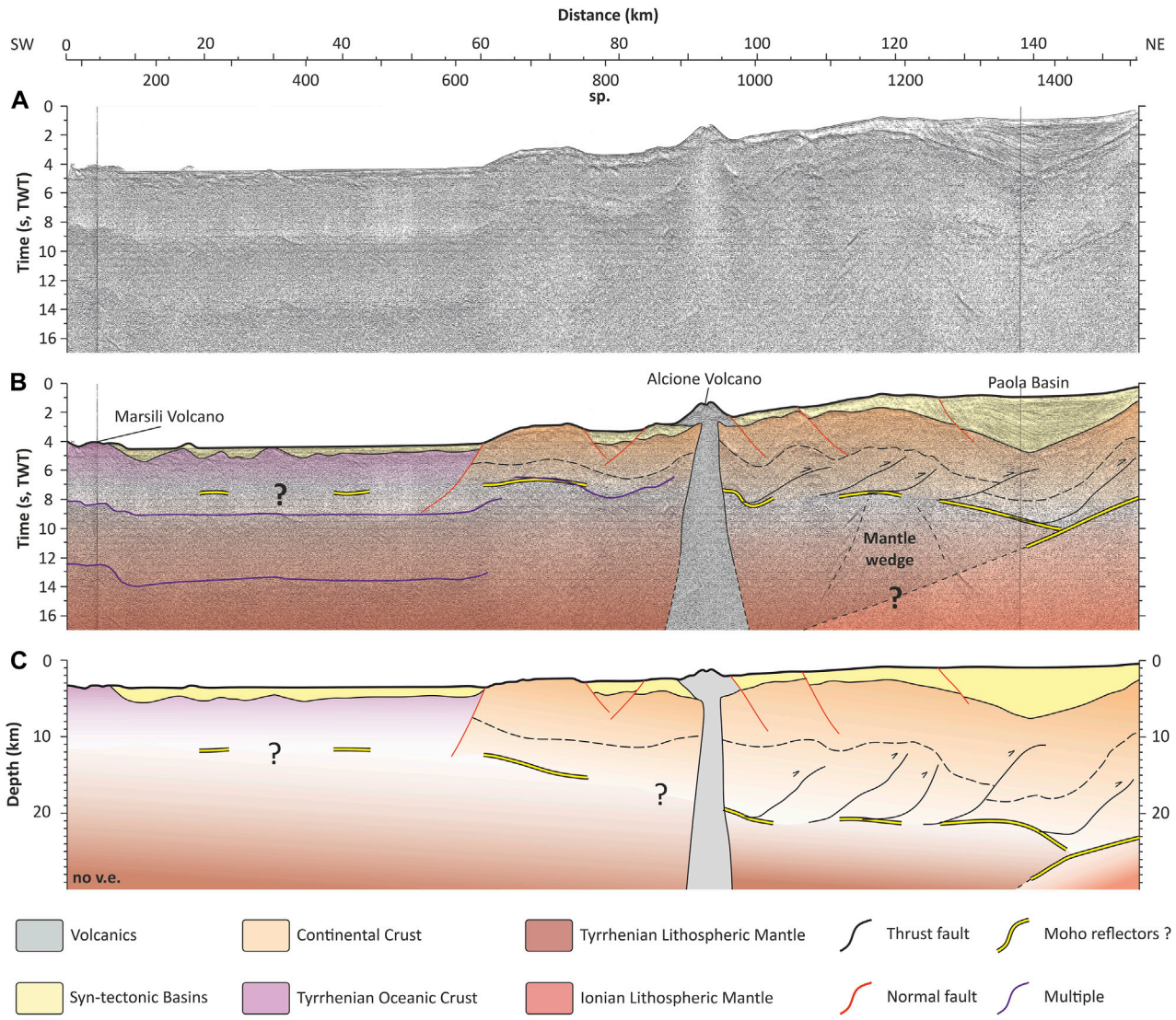

FIGURE 5
Interpreted M27 CROP NVR profile in time clean **(A)** and interpreted **(B)** and depth converted domains **(C)**.

previous seismic reflection surveys (Cernobori et al., 1996). At the SE end of the profile, the top of the old Ionian crust is interpreted at a depth of 7.5 s (TWT) from a series of strong reflectors which progressively deepen North-westwards reaching the depth of 9.5 s TWT in the NW. Due to limited coverage of the available Bouguer gravity anomaly data (Figure 2) our forward modelling is truncated at km 100 of this profile.

In general, the profile does not provide a continuous and convincing image of the Moho discontinuity, which is partly masked by the presence of multiples at the same depth range. Indeed, only a few discontinuous packages of high amplitude low-frequency reflectors could be recognised and interpreted as the Moho discontinuity.

4.2 M27 and M2AA CROP profiles

The M27 (Figure 5) and M2A/III (Figure 6) profiles, acquired in the Tyrrhenian Sea offshore Calabria with a SW-NE and NW-SE trend, respectively, show the Tyrrhenian upper plate region of the TCISS. The tectono-stratigraphic interpretation of these two lines provides important constraints on the thickness and arrangement of the main tectonic and structural elements of the Tyrrhenian margin of the Calabrian Arc.

4.2.1 M27 profile

The M27 profile (Figure 5) images several tectono-stratigraphic features (or domains) that typically develop along subduction zones. At the NW edge of the profile (sp. 90–150), a series of chaotic reflectors are related to the volcanic material of the Marsili seamount. Further to the east (sp. 150–630), a series of high-amplitude low-frequency reflectors are interpreted to be the seismic signature of the Tyrrhenian oceanic crust. The oceanic crust is topped by a thin (0.5–1.5 km) sedimentary cover, characterised by high-amplitude and continuous reflectors. Between sp. 630 and 960, the profile images the submarine Alcione volcano, which is part of the Aeolian volcanic arc (Lucchi et al., 2013). In the eastern part of the profile, the Paola basin is well-illuminated, and it is characterized by well-defined high amplitude sub-parallel continuous

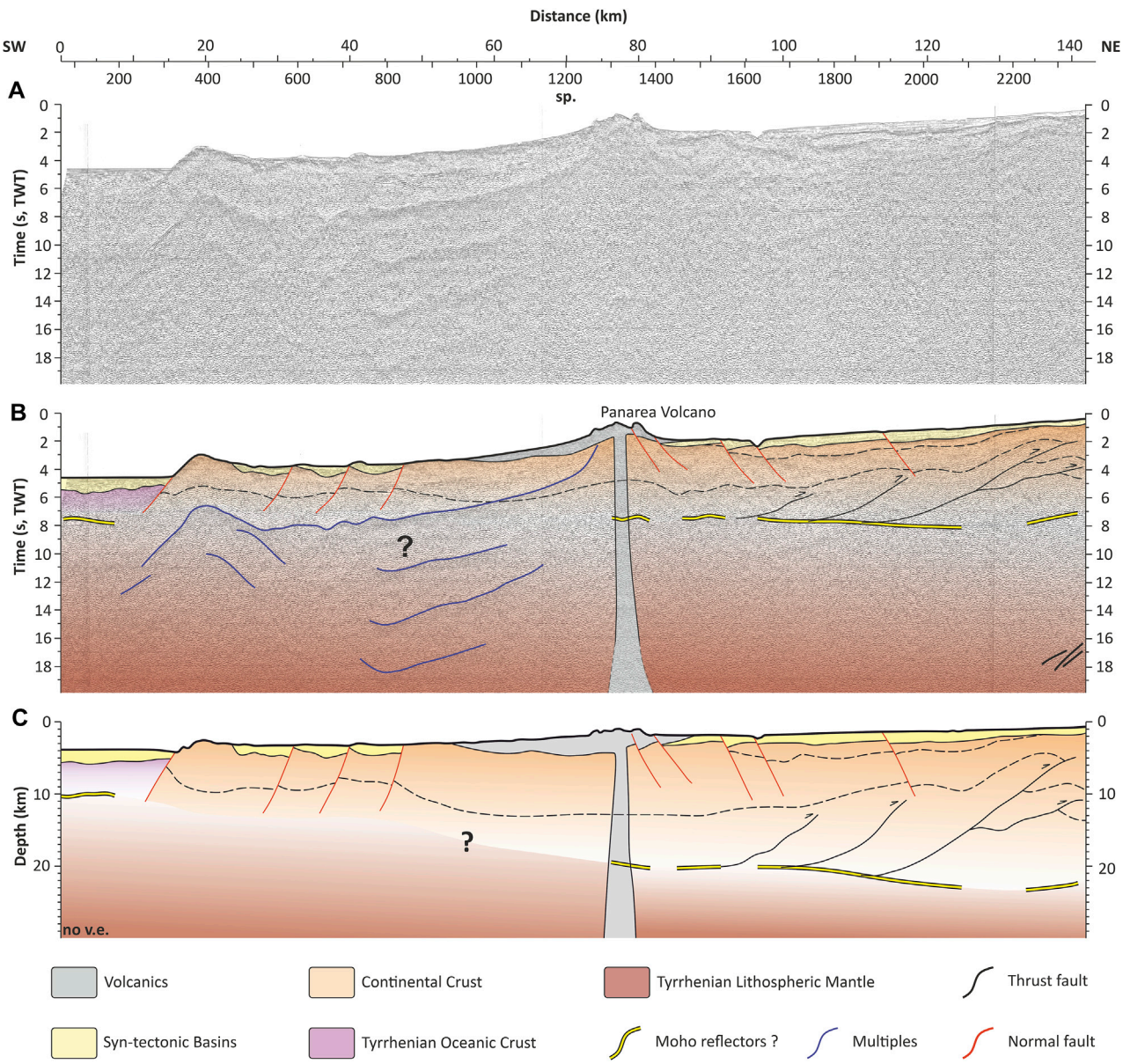

FIGURE 6
Interpreted M27 CROP NVR profile in time clean **(A)** and interpreted **(B)** and depth converted domains **(C)**.

reflectors that can be interpreted as ~5 km thick Pliocene–Quaternary sedimentary deposits (Monaco et al., 1996; Pepe et al., 2010).

Between sp. 200 and 500, at around 7 s (TWT), the almost flat Tyrrhenian Moho is detectable even if it appears not continuous. Between sp. 630 and 1,400, high-amplitude low-frequency reflectors of the Tyrrhenian Moho are more evident, becoming progressively deeper eastwards, reaching about 11 s (TWT) beneath the depocenter of the Paola basin.

Between sp. 1,350 and 1,500, a prominent west-dipping reflector (8–11 s TWT) could be the seismic expression of the subducting Ionian Moho. Further, a series of diffractions recognized at around 8 s (TWT) beneath the western edge of the Paola basin, could be attributed to an uprising, fluids-rich portion of the Tyrrhenian lithospheric mantle.

4.2.2 M2A/III profile

In the NW part of the profile (sp. 90–310), a 8 km thick Tyrrhenian oceanic crust is clearly imaged by high-amplitude low-frequency reflectors (Figure 6). The oceanic crust is overlain by a 1.5 km thick sedimentary cover, characterised by a series of high-amplitude and continuous reflectors. The transition from the oceanic to the continental crust is marked by a series of W-dipping normal faults. Between sp. 950 and 1,500, a series of chaotic reflectors are interpreted as volcanic material associated with the Panarea volcano.

At depth, the reflectors of the Tyrrhenian Moho are not clearly detectable in the NW part of the profile beneath the young oceanic crust. A more evident Moho image can be associated with high-amplitude low-frequency reflectors at 8 s (TWT), between sp. 1950 and 2050. Between sp. 2,150 and 2,350, a series of SW-

TABLE 1 Seismic velocities (m/s) compiled from literature compared with the present study.

	Scarascia et al. (1994)	Neri et al. (2009)	Pepe et al. (2010)	Polonia et al. (2011)	Dellong et al. (2018)	Scarfi et al. (2018)	Present study
Syn-tectonic unit	<6.0	4.5–5.3	2.1	—	2.0–2.35	—	3.2
Messinian evaporites	—	—	—	4–5	4.5–4.8	—	
Volcanic bodies	—	—	5.5	—	—	—	5.5
Upper crust	6–6.3	5.7–6.5	5.5–6	—	5.5	5.7–6.2	6.5
Lower crust	6.5–7.3	6.5–7	6.5–7.5	—	6.6	6.5–7	
Oceanic crust	—	—	—	—	6.5–7.4	7.5	7
New Oceanic crust	—	—	—	—	—	—	6.6
Upper mantle	8	—	—	—	—	7.8–8	8.1

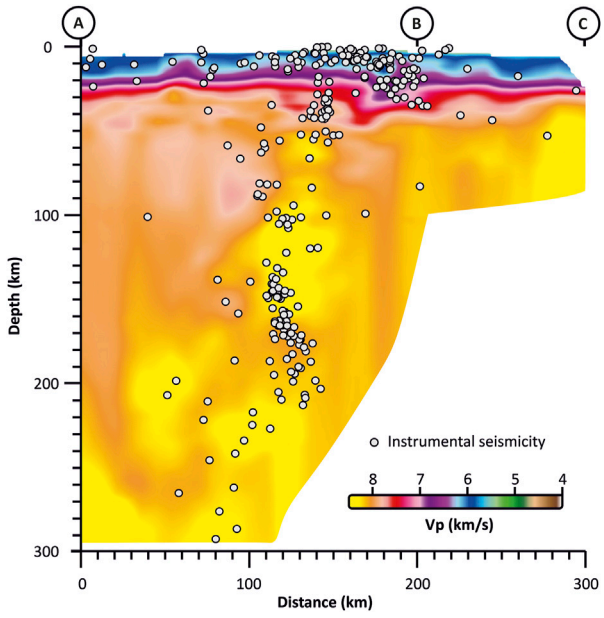

FIGURE 7
Tomographic modelling and seismicity distribution along the study profile (after Scarfi et al., 2018).

dipping high-amplitude subparallel reflectors (16–18 s TWT) might correspond to the top of the Ionian subducting slab.

5 Lithosphere tomography and seismicity distribution

5.1 Lithospehere Vp tomography

Figure 7 shows a NW-SE trending vertical section of the tomographic V_P model by Scarfi et al. (2018), effectively imaging the deep architecture of the TCISS, along the transect modelled in this work (see trace in Figure 1). The descending slab is clearly depicted by the tomographic image, confirming the overall geometry depicted by deeper tomographic models of the mantle (e.g., Dellong et al., 2020): in fact, the sub-vertical (more than 70°) high-velocity anomaly (V_P > 8.4 km/s), that goes down through the mantle from about 50 to 300 km of depth, can be interpreted as a cold oceanic lithosphere that penetrates a warmer and lower velocity supra-subduction lithospheric mantle and asthenosphere. Accordingly, an NW subducting slab geometry is imaged to be continuous at least up to 300 km in the considered section.

The V_P model of Figure 7 also well delineates the lateral variations of the Moho depth across the TCISS; a relatively thin crust characterises both the upper and the lower plates under the Tyrrhenian and external Ionian Sea, respectively. A thicker crustal wedge (down to about 50 km of depth) is instead identified beneath the inner portion of the Ionian accretionary wedge and below the Calabrian backstop. P-wave velocities higher than >6 km/s are found in the continental crust beneath the Calabrian Arc in the depth range of 10–15 km.

In the western sector of the section, a strong negative velocity anomaly, wedging up from the bottom of the Tyrrhenian thinned crust, suggests mantle upwelling below the Aeolian volcanic arc (Ventura, 2013).

5.2 Seismicity distribution (the Ionian Wadati-Benioff zone)

The geometry and structure of the subduction zone are further constrained by the large available dataset of shallow and deep earthquakes (see Scarfi et al., 2018), also plotted along the same profile (Figure 7). Intermediate and deep earthquakes, which are located within the positive seismic velocity anomalies in the upper mantle, reveal the plate interactions and allow to map a very steep (>70°) Wadati-Benioff zone (Figure 7). In a more general view, the slab geometry can be deduced by the deep seismicity distribution,

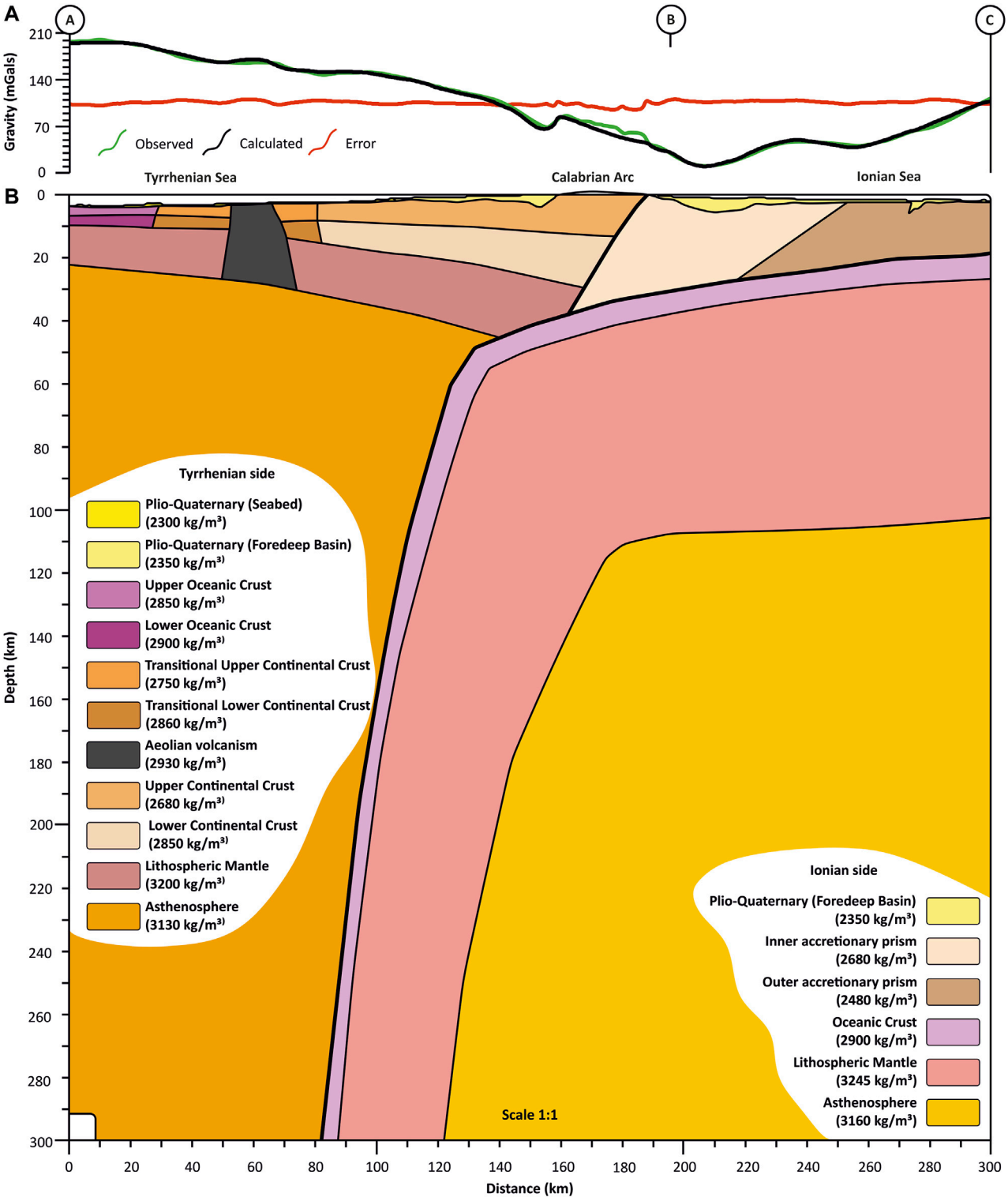

FIGURE 8
Integrated best-fitting Bouguer gravity forward model across the study profile. **(A)** Comparison between observed (black line) and calculated anomaly (green line) **(B)** synthetic model across the investigated profile at 1:1 scale. Density of the modelled blocks was assigned according to colour-coded units.

registered in the SE sector of the Tyrrhenian Sea, according to a trend following the western Calabrian coastline (see Figure 1). Shallower seismicity is instead mostly located within the inner portion of the Calabrian accretionary wedge, with a trend that highlights a deepening of the foci towards SE (see also Barreca et al., 2021).

Historical seismicity testifies that the region has been the site of numerous destructive earthquakes (Rovida et al., 2022; Polonia et al.,

2023). The analysis of the instrumental seismicity at the regional scale reveals that the Calabrian Arc is affected by a prevailing extensional regime, while the accretionary wedge area is affected by a stress field characterized by sub-horizontal P-axes striking roughly NW-SE (see Scarfì et al., 2021).

6 Forward modelling of Bouguer anomalies

6.1 Observed Bouguer gravity anomalies along the study transect

Gravity forward modelling was performed along NNW-SSE trending, 290 km long transect across the whole TCISS, from the Tyrrhenian back-arc basin to the Ionian oceanic basin, extended down to 300 km depth (Figure 8).

Across the study area in Figure 2A, the Bouguer gravity anomaly ranges between 8 and 220 mGal. The anomaly maxima, an almost flat segment of ca. 200 mGal, is located in the central part of the Southern Tyrrhenian Sea oceanic floor (Marsili basin, Scarascia et al., 1994), reflecting the presence of dense, newly-formed oceanic crust, confirmed by its magnetic signature (Nicolosi et al., 2006) and drilled wells (Kastens, 1988; Kastens and Mascle 1990). Moving progressively eastward, Bouguer anomaly values decrease towards the peri-Tyrrhenian continental platform margin and to the onshore Calabrian Mountain range. The Bouguer minima, resembling an arc-shaped feature, extend from the NW-SE trending Neogene clastic continental basins of Southern Italy to the marine wedge-top basins of the Ionian side of Calabria. On the eastern part of the map, gravity values gradually increase south-eastwards, approaching the abyssal plain of the Ionian Sea.

The gravity patterns described above are well reflected in the gravity profile along the study transect (Figure 2B). In the Southern Tyrrhenian Sea, the maximum gravity value is 198 mGals. The gravity minimum is observed in the central part of the modelled transect with values of 8 mGals. Bouguer gravity increases, reaching 108 mGals at the southeastern end of the modelled profile.

6.2 Gravity model of the lithospheric transect

Starting from the Bouguer anomaly data (Figure 2) along the modelled profile, we propose the best-fitting forward gravity model shown in Figure 8.

The model represents a 290 km-long and 300 km-deep volume imaging the complete TCISS, and crossing, from SE to NW: the wide accretionary wedge across the Ionian Sea; the Calabrian-Peloritan onshore continental block and its western, thinned margin; The Paola forearc basin; the Aeolian volcanic arc; and the Marsili basin in the Southern Tyrrhenian back-arc. The geometries of the synthetic blocks included in the model presented in Figure 8, have been constrained by integrating different data sources, i.e., the available literature data about Moho discontinuities and passive seismic data (see Section 3), the reinterpreted deep seismic profiles (see Section 4), and a tomographic model matching the location of the modelled profile (see Section 5).

The density values assigned to the synthetic blocks in Figure 8 were defined according to the pertaining structural domain, as derived after seismic interpretations and tomography data, and by comparison with the density data available in the literature, as summarised in Table 2. Such data provided starting values for the modelled synthetic blocks, whose density was slightly adjusted in order to fit the observed gravity signature. Table 2 provides the best-fitting density values used in the modelling.

Pliocene-Quaternary sediments infill the shallower, recent basins of both the Tyrrhenian and Ionian Seas, representing the shallowest modelled bodies, including the Squillace basin, reaching a maximum depth of 4.5 km and seabed sediments on the Ionian side of Calabria, and the Paola fore-arc basin, with a maximum depth of 5 km, in the Tyrrhenian side. For all these bodies, a density value between 2,300 and 2,350 kg m^{-3} was assigned, the lower values are found in the Tyrrhenian seabed sediments, with a thickness ranging between 600 and 1,200 m (Akimbekova et al., 2021).

Moving towards deeper layers, different density values were assigned, considering their different tectonic domains. At the north-western end of the transect, starting from the Tyrrhenian domain, we model a ~7 km-thick Tyrrhenian oceanic crust with a density of 2,900 kg m^{-3}.

Further lateral variations were introduced in the peri-Tyrrhenian region, corresponding to the continental margin and platform (between 72 and 151 km of the modelled profile). Here the modelled upper and lower crusts represent the transitional zone between the higher-density Tyrrhenian oceanic crust and the lower densities of the continental Calabrian crust. In this transitional domain, we modelled densities of 2,750 and 2,860 kg m^{-3} for the upper and lower crust, respectively, with a total maximum thickness of 15 km. The density values for transitional upper and lower crusts were adjusted from those modelled by Akimbekova et al. (2021) in the Central Tyrrhenian Sea. Moreover, the transitional crustal volume is affected by magmatic upwelling, related to the Aeolian volcanic Arc, which was modelled with a density of 2,930 kg m^{-3} (Pepe et al., 2010; Tassis et al., 2013).

The forearc Paola basin was modelled as an eastward-thickening block between the Aeolian Volcanic Arc and the Calabrian-Peloritan onshore with maximum thicknesses of 5 km and using a density for the Pliocene-Quaternary sediments of 2,350 kg m^{-3} (Pepe et al., 2010). These shallow basins, allocating the lowest modelled densities in small-sized and thick blocks, carry the shallower and shorter-wavelength sources of the observed Bouguer gravity anomaly as clearly observable between km 140 and 150 and between km 180 and 220 of the modelled profile (Figure 8).

Moving further to the East in the onshore area, we modelled the Calabrian continental crust with a maximum thickness of 29.5 km. Here, the upper crust was attributed with metamorphic and intrusive rocks in the Variscan basement and thus modelled with a density of 2,680 kg m^{-3}, while the lower crust was modelled with a density of 2,850 kg m^{-3}. Modelling of the onshore area was also constrained by outcrops pertaining to the hanging wall of the Ionian subduction (Ortolano et al., 2005; 2015). These hanging wall crustal units are bounded eastward by a major tectonic boundary. This boundary corresponds to the backstop, and merges upwards into a complex thrust system, overlaying the footwall crust, represented by the oceanic Ionian crust. The Ionian oceanic plate is composed of a

10.3389/feart.2023.1259831

TABLE 2 Compilation of the density values (g/cm^3) extracted from the available literature and . summary of the representative density values of the main layers derived in this work from the Bouguer gravity forward modelling.

			Menardi Noguera and Rea (2000)	Tiberti et al. (2005)	Anelli et al. (2007)	Biella et al. (2007)	Pepe et al. (2010)	Tassis et al. (2013)	Dellong et al. (2020)	Mancinelli et al. (2019)	Akimbekova et al. (2021)	Present study
Plio-Quaternary sediments	Thyrrenhian Seabed		2.35	2.3	2.35	—	2.2–2.35	2.2–2.3	2.3	—	2.3	2.3
	Foredeep, wedge-top											2.35
Messinian Evaporites			—	—	—	—	—	—	2.58	—	—	-
Volcanics			—	—	—	—	2.86	3–3.3	—	—	—	2.93
Continental crust	Tyrrhenian	Upper	2.63	2.63–2.65	2.58–2.67	2.6–2.65	2.69	2.75–2.77	2.63	2.58–2.67	2.6–2.65	2.68
		Lower										2.85
	Ionian	Inner wedge										2.68
		Outer wedge										2.48
Transitional crust	Upper		—	—	—	—	—	—	—	—	—	2.75
	Lower											2.86
Oceanic crust	Tyrrhenian	Upper	—	—	—	—	2.85	3	2.8	—	2.85	2.85
		Lower									2.9	2.9
	Ionian		—	—	—	—	3.1	—	—	—	—	2.9
Lithospheric mantle	Tyrrhenian		3.2	3.32	2.95	3.15	3.28–3.37	3.3	3.22	3.2	3.2	3.2
	Ionian				3.1				3.35		3.3	3.24
Asthenosphere	Tyrrhenian		—	—	—	—	3.18–3.34	—	—	—	3.13	3.13
	Ionian											3.16

thin and dense oceanic crust with a maximum thickness of 7 km and a density of 2,900 kg m^{-3}, overlain by a thick accretionary wedge. Such accretionary wedge consists of a mixed lithological assemblage comprising Messinian evaporites, pre-Messinian Miocene deposits, Mesozoic platform, and deep-water pelagic carbonates (Finetti, 2005; Minelli and Faccenna, 2010; Polonia et al., 2011; Gutscher et al., 2017; Maesano et al., 2017). The inner accretionary wedge is thicker, with a maximum thickness of 38 km (between km 156 and 245 in the modelled profile, Figure 8), and is split into two blocks with different densities. The inner accretionary block was modelled with an average density of 2,680 kg m^{-3} representing the crustal rocks of the Ionian slab (Polonia et al., 2011). The outer Accretionary prism was modelled with an average density of 2,480 kg m^{-3}.

In the model, we present two different Moho discontinuities: a newly-formed Tyrrhenian Moho and an older Ionian Moho. In the western end of the modelled profile, the relatively shallow Tyrrhenian Moho, flattening at about 11 km depth, reflects the presence of a deep marine basin (about 3,500 m b.s.l.). In the eastern end, the Ionian Moho is at a depth of ~27 km. In the central part of the profile, beneath the Tyrrhenian coastline, we found the superposition between a gently east-dipping Tyrrhenian Moho at about ~30 km and a deeper and steeper, west-dipping Ionian Moho, intersecting at a depth of ~55 km resembling the subducting slab. The downward continuation of this slab is clearly imaged by deep seismicity (Latorre et al., 2023), as well as by mantle tomography (Scarfì et al., 2021), down to a depth of at least 300 km (Figure 7).

The subducting Ionian mantle was modelled with a density of 3,245 kg m^{-3} beneath the Calabrian and Peloritan continental blocks coastline.

Beneath the Tyrrhenian and the Ionian Moho, the Lithospheric Mantle was also modelled, accounting for different ages and thermal states between the Tyrrhenian and the Ionian domains. In fact, the older and colder Ionian lithospheric mantle was modelled with the relatively higher density value of 3,245 kg m^{-3}, with respect to the presumably hotter and lighter, newly formed Tyrrhenian lithospheric mantle that was modelled with a density of 3,200 kg m^{-3}.

The presence of the uppermost asthenosphere is marked as a lower density (3,130 kg m^{-3}) block found at 20 km depth beneath the Tyrrhenian Sea at the NW end of the profile and intersecting the subducting slab at a depth of 48 km (at km 140 along the modelled profile). Under the Ionian domain, the transition between the asthenosphere and the lithosphere was modelled at ca. 100 km depth, attributing a density value of 3,160 kg m^{-3} to the Ionian asthenosphere, slightly higher than the Tyrrhenian.

7 Discussion and concluding remarks

Considering all the available geophysical and geological constraints, we forward-modelled the Bouguer gravity anomaly along a regional-scale transect spanning from the Tyrrhenian to the Ionian oceanic crusts, cross-cutting the Calabrian Arc. The resulting 290 km-long and 300 km-deep model provides further constraints to the regional lithospheric geometries. Supported by the interpretation and depth conversion of crustal-scale seismic profiles from the CROP project (Scrocca et al., 2003) and by a tomographic model (Scarfì et al., 2018) across the same modelled profile.

The aforementioned multidisciplinary approach was aimed at minimising the intrinsic non-uniqueness that the forward geophysical modelling carries. Nevertheless, we stress that in the workflow we followed, relevant uncertainties can mainly arise from interpretative or procedural errors in the seismic and/or tomographic models. Absolute values and regional trends of the Bouguer gravity signature are clearly affected by the crustal and lithospheric thickness representing the first-order contributor across the entire profile. Density changes between the Ionian and Tyrrhenian lithospheric mantle and asthenosphere were introduced due to the different ages and thermal evolution of the two distinct geodynamic domains. Volcanic intrusions in the younger Tyrrhenian domain also contribute to the observed gravity signature, while the short-wavelength, local-scale gravity anomalies are clearly generated by the shallow, recent basins, such as the Paola and Squillace basins. The crustal setup carries strong lateral density changes, which are found in both the continental and transitional domains. Such lateral contrasts are coherent with the present-day tectonic setting, which is in turn, inherited from the complex geodynamic evolution of the area. A clear example is provided by the mantle upwelling in the Tyrrhenian domain, where it is preceded by lower-density oceanic crust and followed by lower-density Peri-Tyrrhenian transitional crust. While a more complex example is found in the central part of the profile where the subduction hanging wall is in lateral continuity with the transitional upper crust westwards and with the accretionary wedge eastwards. However, to improve the resolution of the upper crustal geometries and density values would require shallower high-quality constraints (boreholes and/or commercial seismic lines) beyond the purpose of this work.

The review of the available literature was both a driver for this work since it highlighted contrasting models for the Moho discontinuities across the area (Figure 3) and was also key for the depth-conversion of the seismic data (Figures 4–6) and for the parametrization of the synthetic blocks in the forward model (Figure 8). Such review allowed us to provide the reader with up-to-date data collection about the average seismic velocities and density values for the study area (Tables 1, 2) and, ultimately, to provide best-fitting density values (Table 2) that are somehow supported by the geometrical references provided by the seismic and tomographic data.

The final forward gravity model (Figure 8) fits the observed gravity field and provides an overall imaging of the TCISS, identifying the first-order geological and geophysical contributors to the observed gravity field. In particular, it effectively images the structural settings of the crust and of the lithospheric mantle along the modelled transect throughout the different structural domains of the Tyrrhenian Neogene oceanic crust, Aeolian Arc, Calabrian continental block and Ionian Mesozoic oceanic crust.

The results of this work will likely contribute also to understanding the lithospheric-scale relationships between depth and seismic velocities and densities by providing reference values for the study area concerning the lithospheric mantle and the lower crust (Tables 1, 2).

Nevertheless, there are still some features that could be furtherly modelled to improve the accuracy and the research

impact of the proposed model. For example, more detailed information on shallow structures can be derived from the interpretation of other seismic reflection profiles, including also high-resolution surveys, acquired offshore (Caporali et al., 2003; 2009; Devoti et al., 2011; D'Agostino et al., 2011b; Carafa et al., 2018; Cambiotti et al., 2020; Gutscher et al., 2017; Dellong et al., 2020). The Moho depth under the Ionian Sea, as well as the mantle rising beneath the Aeolian Arc, also needs some improvement due to the limited resolution of the CROP seismic profiles, especially in their deeper portion. Moreover, future modelling efforts should consider alternative scenarios of the slab geometry, such as the potential occurrence of slab detachment phenomena at intermediate depths. In our current model, we assumed a continuous slab extending at least 300 km, a configuration supported by tomographic imaging and deep seismicity studies (Scarfì et al., 2018; Dellong et al., 2020; Latore et al., 2023). Scarfì et al. (2018) propose a comprehensive 3D image of the Calabro-Ionian subduction system in the central Mediterranean, obtained through seismic tomography and integrated with earthquake data. Their findings indicate that the slab remains continuous beneath the southern sector of the Calabro-Peloritan Arc where our profile is crossing. However, deformation processes occurring at its edges contribute to its gradual narrowing. Combined analysis of tomography and earthquake distribution suggests that the slab is continuous only in its SW part (From ATLFS to the Gulf of S. Eufemia). This long-lasting (35 Ma) NW-dipping subduction of the ancient Ionian oceanic lithosphere affects surface tectonics and magmatism, potentially leading to stress concentration in the tip zones. The authors identify three distinct seismogenic zones, with our model profile crossing between zone 3 (the slab) and zone 2 (a tear fault bounding the slab SW), referred to as the "Aeolian Tindari Letojanni Fault System" (ATLFS). Latorre et al. (2023) analyze the CLASS catalogue of earthquakes, where the Ionian slab is imaged by the seismicity distribution. A near-vertical Benioff-Wadati zone (>75°) at a depth of 80–300 km between the Aeolian Arc and the submerged Paola forearc basin. Also, in this work, the slab is continuous only in the "central" part of the study area, and the section highlights that the shallow part of the slab (D<80 km) dips 55°, whilst the deeper part is nearly vertical (>75°). Dellong et al. (2020) image the slab and related seismicity that reaches a depth of about 500 km.

An important extension of this research, which could be beneficial for both the scientific community and society, should be focused on providing a more comprehensive understanding of the natural hazards associated with the region. This includes further studies of the active tectonics of the region concerning geodetic data (Billi et al., 2023), that can provide valuable insights into the ongoing processes of plate collision and subduction. Such studies would provide the base for a revision of the crustal-scale seismotectonics of this region including its eventual potential to generate megathrust events. In this frame, the compressional seismicity at the crustal-scale, with particular focus on the lower crust and the accretionary wedge, is still poorly understood and represents an important area of research that can help us to better understand the present-day dynamics of this complex region and possibly locate crustal volumes that are prone to strong compressional seismicity.

Being constrained by seismic reflection data (Figures 4–6) and in agreement with previous models in the available literature (Figure 3), our modelling provides the first-order lithospheric-scale tomographic (Figure 7) and geometric (Figure 8) constraints where such studies can be framed.

Finally, the key findings of this work can be summarised as follows:

1. Basin gravity signatures: The Calabrian arc is flanked by two prominent recent basins that carry clear and strong short-wavelength gravity signatures, i.e., the Paola forearc basin in the hinterland, the wider and deeper Squillace basin on top of the accretionary wedge.
2. Tectonic complexity: The orogen displays a heterogeneous nature and complex arrangement of the involved tectonic units. The lateral complexity of the upper crust contributes to the observed gravity signature through strong lateral density contrasts ranging from the transitional crust (separating the Calabrian Arc from the Tyrrhenian young oceanic crust) in the Tyrrhenian domain, to the thick and wide accretionary wedge covering the old oceanic crust of the in the Ionian domain.
3. Accretionary wedge: A well-developed, thick Accretionary prism is present in the Ionian Sea and its thickness and density decrease eastward, compatibly with the observed gravity signature.
4. Crustal Structure: Two distinct, superposed Moho discontinuities can be modeled across the Calabrian Arc. The footwall plate displays a subducting, westward-dipping Ionian Moho of older late Paleozoic-Mesozoic origin, while the hanging wall plate showcases a newly-formed Neogene Tyrrhenian Moho.
5. Heterogeneities at the asthenospheric scale: The observed Bouguer gravity anomaly is compatible with slight density differences between the Tyrrhenian and the Ionian domains, supporting different ages and thermal evolutions of the two.
6. Ongoing Subduction: In the Calabrian Arc, the subduction of the Ionian oceanic lithosphere appears to be active, as evidenced by well-developed deep seismicity extending to at least 300 km (Figure 7; Scarfì et al., 2019; Latorre et al., 2023).
7. Subduction-Related Volcanism: The Aeolian volcanic arc exhibits clear evidence of subduction-related volcanism (Lucchi et al., 2013; Ventura, 2013; Castro-Melgar et al., 2021), that is compatible with the observed gravity signature (Figure 8).

These findings contribute to our understanding of the orogen's morphology and of its tectonic and geodynamic evolution by providing new evidence on the size and extent of the main basins, the crustal structure and the volcanic activity in the Aeolian arc. Finally, these findings provide valuable insights into the dynamic processes shaping the region and have implications for seismic hazard assessment and geological modelling in similar tectonic settings.

We believe that this model will contribute to the tectonic and geodynamic understanding of this intriguing and complex region, towards the refinement of the seismogenic crustal thickness and possibly assessing the potential of this subducting zone to generate megathrust earthquakes.

Data availability statement

The datasets presented in this article are not readily available because the Gravity data was given by third parties and cannot be further distributed. Requests to access the datasets should be directed to asselakimbekova@gmail.com.

Author contributions

AA: Data curation, Investigation, Methodology, Software, Writing–original draft, Writing–review and editing. FC: Data curation, Resources, Software, Visualization, Writing–review and editing. PM: Methodology, Software, Supervision, Writing–review and editing. GB: Conceptualization, Formal Analysis, Supervision, Validation, Writing–review and editing. LS: Formal Analysis, Investigation, Methodology, Resources, Software, Visualization, Writing–review and editing. CP: Conceptualization, Methodology, Project administration, Software, Writing–review and editing. CM: Formal Analysis, Resources, Validation, Writing–review and editing. MB: Conceptualization, Formal Analysis, Funding acquisition, Investigation, Methodology, Project administration, Supervision, Validation, Writing–review and editing.

Funding

The author(s) declare financial support was received for the research, authorship, and/or publication of this article. This research is part of the MUSE-4D project, financed by MUR in the framework of PRIN-2017 (project #2017KT2MKE_003): U.R Responsible MB, National P.I. G. Lavecchia.

Acknowledgments

We thank ENI S.p.A. for providing the gravity data used in this work: the data were provided under a specific agreement with the Dipartimento di Fisica e Geologia of Perugia University and cannot be redistributed to third parties. The seismic interpretation and depth conversion was performed using Move software (Petroleum Experts).

Conflict of interest

The authors declare that the research was conducted in the absence of any commercial or financial relationships that could be construed as a potential conflict of interest.

Publisher's note

References

Akimbekova, A., Mancinelli, P., Pauselli, C., Minelli, G., and Rinaldo Barchi, M. (2021). Forward modelling of bouguer anomalies along a transect of the southern apennines and the southern Tyrrhenian Sea (Italy). *Italian J. Geosciences* 140 (3), 411–421. doi:10.3301/ijg.2021.03

Amodio-Morelli, L., Bonardi, G., Colonnna, V., Dietrich, D., Giunta, G., Ippolito, F., et al. (1976). L'Arco calabro-peloritano nell'Orogene appenninico-maghrebide. *Mem. Soc. Geol. Ital.* 17, 1–60.

Anelli, L., Cappelli, V., Cassano, E., Giori, I., and Torre, P. L. (2007). Integrated interpretation of the magnetic and gravity data along the seismic line CROP-04. *Boll. Soc. Geol. It. (Ital. J. Geosci.)* 7, 257–266.

Barreca, G., Bruno, V., Cultrera, F., Mattia, M., Monaco, C., and Scarfì, L. (2014). New insights in the geodynamics of the Lipari–Vulcano area (Aeolian Archipelago, southern Italy) from geological, geodetic and seismological data. *J. Geodyn.* 82, 150–167. doi:10.1016/j.jog.2014.07.003

Barreca, G., Gross, F., Scarfì, L., Aloisi, M., Monaco, C., and Krastel, S. (2021). The Strait of Messina: seismotectonics and the source of the 1908 earthquake. *Earth-Science Rev.* 218, 103685. doi:10.1016/j.earscirev.2021.103685

Barreca, G., Scarfì, L., Gross, F., Monaco, C., and De Guidi, G. (2019). Fault pattern and seismotectonic potential at the south-western edge of the Ionian subduction system (southern Italy): new field and geophysical constraints. *Tectonophysics* 761, 31–45. doi:10.1016/j.tecto.2019.04.020

Bassett, D., and Watts, A. B. (2015). Gravity anomalies, crustal structure, and seismicity at subduction zones: 1. Seafloor roughness and subducting relief. *Geochem. Geophys. Geosyst.* 16, 1508–1540. doi:10.1002/2014GC005684

Ben-Avraham, Z., and Grasso, M. (1991). Crustal structure variations and transcurrent faulting at the eastern and western margins of the eastern Mediterranean. *Tectonophysics* 196 (3-4), 269–277. doi:10.1016/0040-1951(91)90326-n

Biella, G., De Franco, R., Marsella, E., and Caielli, G. (2007). Deep structures in Southern Italy. Evidences from the Gargano-Pantelleria seismic refraction experiment (1971). *Boll. Soc. Geol. It., Suppl.* 7, 163–175.

Billi, A., Cuffaro, M., Orecchio, B., Palano, M., Presti, D., and Totaro, C. (2023). Retracing the Africa–Eurasia nascent convergent boundary in the Western Mediterranean based on earthquake and GNSS data. *Earth Planet. Sci. Lett.* 601, 117906. doi:10.1016/j.epsl.2022.117906

Calò, M., Dorbath, C., Luzio, D., Rotolo, S. G., and D'Anna, G. (2012). Seismic velocity structures of Southern Italy from tomographic imaging of the Ionian slab and petrological inferences. *Geophys. J. Int.* 191 (2), 751–764. doi:10.1111/j.1365-246X.2012.05647.x

Cambiotti, G., Palano, M., Orecchio, B., Marotta, A. M., Barzaghi, R., Neri, G., et al. (2020). New insights into long-term aseismic deformation and regional strain rates from GNSS data inversion: the case of the pollino and castrovillari faults. *Remote Sens.* 12 (18), 2921. doi:10.3390/rs12182921

Caporali, A., Aichhorn, C., Barlik, M., Becker, M., Fejes, I., Gerhatova, L., et al. (2009). Surface kinematics in the Alpine–Carpathian–Dinaric and Balkan region inferred from a new multi-network GPS combination solution. *Tectonophysics* 474 (1-2), 295–321. doi:10.1016/j.tecto.2009.04.035

Caporali, A., Martin, S., and Massironi, M. (2003). Average strain rate in the Italian crust inferred from a permanent GPS network–II. Strain rate versus seismicity and structural geology. *Geophys. J. Int.* 155 (1), 254–268. doi:10.1046/j.1365-246x.2003.02035.x

Carafa, M. M. C., Kastelic, V., Bird, P., Maesano, F. E., and Valensise, G. (2018). A "Geodetic Gap" in the Calabrian Arc: evidence for a locked subduction megathrust? *Geophys. Res. Lett.* 45 (4), 1794–1804. doi:10.1002/2017gl076554

Casero, P., Cita, M. B., Croce, M., and De Micheli, A. (1984). Tentativo di interpretazione evolutiva della scarpata di Malta basata su dati geologici e geo®sici. *Mem. Soc. Geol. It.* 27, 233–253.

Cassinis, R., Scarascia, S., and Lozej, A. (2003). The deep crustal structure of Italy and surrounding areas from seismic refraction data. A new synthesis. *Boll. della Soc. Geol. Ital.* 122, 365–376.

Castro-Melgar, I., Prudencio, J., Del Pezzo, E., Giampiccolo, E., and Ibáñez, J. M. (2021). Shallow magma storage beneath Mt. Etna: evidence from new attenuation tomography and existing velocity models. *J. Geophys. Res. Solid Earth* 126, e2021JB022094. doi:10.1029/2021JB022094

Catalano, R., Doglioni, C., and Merlini, S. (2001). On the mesozoic Ionian Basin. *Geophys. J. Int.* 144, 49–64. doi:10.1046/j.0956-540x.2000.01287.x

Cernobori, L., Hirn, A., McBride, J. H., Nicolich, R., Petronio, L., Romanelli, M., and STREAMERS/PROFILES Working Groups (1996). Crustal image of the Ionian Basin and its calabrian margins. *Tectonophysics* 264, 175–189. doi:10.1016/s0040-1951(96)00125-4

Cultrera, F., Barreca, G., Ferranti, L., Monaco, C., Pepe, F., Passaro, S., et al. (2017). Structural architecture and active deformation pattern in the northern sector of the Aeolian-Tindari-Letojanni fault system (SE Tyrrhenian Sea-NE Sicily) from integrated analysis of field, marine geophysical, seismological and geodetic data. *Ital. J. Geosci.* 136, 399–417. doi:10.3301/IJG.2016.17

D'Agostino, N., D'Anastasio, E., Gersavi, A., Guerra, I., Nedimović, M. R., Seeber, L., et al. (2011b). Forearc extension and slow rollback of the Calabrian Arc from GPS measurements. *Geophys. Res. Lett.* 38, L17304. doi:10.1029/2011GL048270

D'Agostino, N., Avallone, A., Cheloni, D., D'Anastasio, E., Mantenuto, S., and Selvaggi, G. (2008). Active tectonics of the Adriatic region from GPS and earthquake slip vectors. *J. Geophys. Res.* 113, B12413. doi:10.1029/2008JB005860

Dannowski, A., Kopp, H., Klingelhoefer, F., Klaeschen, D., Gutscher, M. A., Krabbenhoeft, A., et al. (2019). Ionian Abyssal Plain: a window into the tethys oceanic lithosphere. *Solid* 10 (2), 447–462. doi:10.5194/se-10-447-2019

De Astis, G., Ventura, G., and Vilardo, G. (2003). Geodynamic significance of the Aeolian volcanism (Southern Tyrrhenian Sea, Italy) in light of structural, seismological, and geochemical data. *Tectonics* 22 (4), 1040. doi:10.1029/2003TC001506

De Voogd, B., Truffert, C., Chamot-Rooke, N., Huchon, P., Lallemant, S., and Le Pichon, X. (1992). Two-ship deep seismic soundings in the basins of the Eastern Mediterranean Sea (Pasiphae cruise). *Geophys. J. Int.* 109, 536–552. doi:10.1111/j.1365-246x.1992.tb00116.x

Dellong, D., Klingelhoefer, F., Dannowski, A., Kopp, H., Murphy, S., Graindorge, D., et al. (2020). Geometry of the deep Calabrian subduction (Central Mediterranean Sea) from wide-angle seismic data and 3-D gravity modeling. *Geochem. Geophys. Geosystems* 21 (3). doi:10.1029/2019gc008586

Dellong, D., Klingelhoefer, F., Kopp, H., Graindorge, D., Margheriti, L., Moretti, M., et al. (2018). Crustal structure of the Ionian basin and eastern Sicily margin: results from a wide-angle seismic survey. *J. Geophys. Res. Solid Earth* 123, 2090–2114. doi:10.1002/2017JB015312

Devoti, R., Esposito, A., Pietrantonio, G., Pisani, A. R., and Riguzzi, F. (2011). Evidence of large scale deformation patterns from GPS data in theItalian subduction boundary. *Earth Planet. Sci. Lett.* 311 (3–4), 230–241. doi:10.1016/j.epsl.2011.09.034

Di Stefano, R., Bianchi, I., Ciaccio, M. G., Carrara, G., and Kissling, E. (2011). Correction to "Three-dimensional Moho topography in Italy: new constraints from receiver functions and controlled source seismology.". *Geochem. Geophys. Geosystems* 12 (12). doi:10.1029/2011gc003967

Engdahl, E. R., van der Hilst, R., and Buland, R. (1998). Global teleseismic earthquake relocation with improved travel times and procedures for depth determination. *Bull. Seismol. Soc. Am.* 88 (3), 722–743. doi:10.1785/bssa0880030722

Fabbri, A., Rossi, S., Sartori, R., and Barone, A. (1982). Evoluzione neogenica dei margini dell'Arco Calabro-Peloritano: implicazini geodinamiche. *Mem. Soc. Geol. It.* 24, 357–366.

Faccenna, C., Becker, T. W., Auer, L., Billi, A., Boschi, L., Brun, J. P., et al. (2014). Mantle dynamics in the mediterranean. *Rev. Geophys.* 52, 283–332. doi:10.1002/2013rg000444

Faccenna, C., Becker, T. W., Lucente, F. P., Jolivet, L., and Rossetti, F. (2001). History of subduction and back arc extension in the Central Mediterranean. *Geophys. J. Int.* 145 (3), 809–820. doi:10.1046/j.0956-540x.2001.01435.x

Faccenna, C., Piromallo, C., Crespo-Blanc, A., Jolivet, L., and Rossetti, F. (2004). Lateral slab deformation and the origin of the western Mediterranean arcs. *Tectonics* 23, TC1012. doi:10.1029/2002tc001488

Ferranti, L., Antonioli, F., Amorosi, A., Dai Prà, G., Mastronuzzi, G., Mauz, B., et al. (2006). Markers of the last interglacial sea-level high stand along the coast of Italy: tectonic implications. *Quat. Int.* 145 (146), 30–54. doi:10.1016/j.quaint.2005.07.009

Finetti, I., Lentini, F., Carbone, S., Catalano, S., and Del Ben, A. (1996). Il sistema appennino meridionale–arco calabro–sicilia nel mediterraneo centrale: studio geologico-geofisico. *Boll. Soc. Geol. It.* 115, 529–559.

Finetti, I. R. (2005). "Depth contour map of the Moho discontinuity in the central mediterranean region from new CROP seismic data," in *CROP project - deep seismic exploration of the mediterranean and Italy*. Editor I. R. Finetti, 597–606. Chap.27.

Finetti, I. (1982). Structure, stratigraphy and evolution of central Mediterranean. *Boll. Geofis. Teor. Appl.* 24, 247–315.

Frepoli, A., Selvaggi, G., Chiarabba, C., and Amato, A. (1996). State of stress in the Southern Tyrrhenian subduction zone from fault-plane solutions. *Geophys. J. Int.* 125, 879–891. doi:10.1111/j.1365-246x.1996.tb06031.x

Frizon de Lamotte, D., Raulin, C., Mouchot, N., Wrobel-Daveau, J. C., Blanpied, C., and Ringenbach, J. C. (2011). The southernmost margin of the Tethys realm during the Mesozoic and Cenozoic: initial geometry and timing of the inversion processes. *Tectonics* 30, TC3002. doi:10.1029/2010TC002691

Gallais, F., Gutscher, M. A., Graindorge, D., Chamot-Rooke, N., and Klaeschen, D. (2011). A Miocene tectonic inversion in the Ionian Sea (central Mediterranean): evidence from multichannel seismic data. *J. Geophys. Res.* 116, B12108. doi:10.1029/2011JB008505

Ghisetti, F., and Vezzani, L. (1982). Different styles of deformation in the calabrian arc (Southern Italy): implications for a seismotectonic zoning. *Tectonophysics* 85 (3–4), 20149–165. doi:10.1016/0040-1951(82)90101-9

Goes, S., Giardini, D., Jenny, S., Hollenstein, C., Kahle, H.-G., and Geiger, A. (2004). A recent tectonic reorganization in the south-central Mediterranean. *Earth Planet. Sci. Lett.* 226, 335–345. doi:10.1016/j.epsl.2004.07.038

Gutscher, M.-A., Dominguez, S., Mercier de Lepinay, B., Pinheiro, L., Gallais, F., Babonneau, N., et al. (2016). Tectonic expression of an active slab tear from high-resolution seismic and bathymetric data offshore Sicily (Ionian Sea). *Tectonics* 34, 39–54. doi:10.1002/2015TC003898

Gutscher, M.-A., Kopp, H., Krastel, S., Bohrmann, G., Garlan, T., Zaragosi, S., et al. (2017). Active tectonics of the Calabrian subduction revealed by new multi-beam bathymetric data and high resolution seismic profiles in the Ionian Sea (Central Mediterranean). *Earth Planet. Sci. Lett.* 461, 61–72. doi:10.1016/j.epsl.2016.12.020

Jacques, E., Monaco, C., Tapponier, P., Tortorici, L., and Winter, T. (2001). Faulting and earthquake triggering during the 1783 Calabria seismic sequence. *Geophys. J. Int.* 147, 499–516. doi:10.1046/j.0956-540x.2001.01518.x

Johnston, S. T., and Mazzoli, S. (2009). "The Calabrian Orocline: buckling of a previously more linear orogen,". *Ancient orogens and modern analogues*. Editors J. B. Murphy, J. D. Keppie, and A. J. Hynes (Geol. Soc., London, Spec. Publ.), 327, 113–125. doi:10.1144/SP327.7

Jolivet, L., and Faccenna, C. (2000). Mediterranean extension and the Africa-Eurasia collision. *Tectonics* 19 (6), 1095–1106. doi:10.1029/2000tc900018

Kastens, K. A. (1988). The case for asymmetrical rifting above a detachment fault in the opening of the Tyrrhenian Sea, central Mediterranean. *EOS* 69, 465.

Kastens, K., and Mascle, J. (Editors) (1990). "The geological evolution of the Tyrrhenian Sea: an introduction to the scientific results of ODP Leg 107,". *Proc. ODP, sci. Results*. (College Station, TX: Ocean Drilling Program), 107, 3–26. doi:10.2973/odp.proc.sr.107.187.1990

Latorre, D., Di Stefano, R., Castello, B., Michele, M., and Chiaraluce, L. (2023). An updated view of the Italian seismicity from probabilistic location in 3D velocity models: the 1981–2018 Italian catalog of absolute earthquake locations (CLASS). *Tectonophysics* 846, 229664. doi:10.1016/j.tecto.2022.229664

F. Lucchi, A. Peccerillo, J. Keller, C. A. Tranne, and P. L. Rossi (Editors) (2013). *The Aeolian islands volcanoes* (Geological Society of London).

Maesano, F. E., Tiberti, M. M., and Basili, R. (2017). The Calabrian Arc: three-dimensional modelling of the subduction interface. *Sci. Rep.* 7 (1), 8887. doi:10.1038/s41598-017-09074-8

Malinverno, A., and Ryan, W. B. F. (1986). Extension in the Tyrrhenian Sea and shortening in the Apennines as result of arc migration driven by sinking of the lithosphere. *Tectonics* 5, 227–245. doi:10.1029/tc005i002p00227

Mancinelli, P., Pauselli, C., Fournier, D., Fedi, M., Minelli, G., and Barchi, M. R. (2020). Three dimensional gravity local inversion across the area struck by the 2016–2017 seismic events in Central Italy. *J. Geophys. Res. Solid Earth* 125 (2), e2019JB018853. doi:10.1029/2019jb018853

Mancinelli, P., Porreca, M., Pauselli, C., Minelli, G., Barchi, M. R., and Speranza, F. (2019). Gravity and Magnetic Modeling of Central Italy: insights into the depth extent of the seismogenic layer. *Geochem. Geophys. Geosystems* 20, 2157–2172. doi:10.1029/2018GC008002

Mancinelli, P., Scisciani, V., Patruno, S., and Minelli, G. (2021). Gravity modeling reveals a messinian foredeep depocenter beneath the intermontane fucino basin (central apennines). *Tectonophysics* 821, 229144. doi:10.1016/j.tecto.2021.229144

Marotta, A. M., Spelta, E., and Rizzetto, C. (2006). Gravity signature of crustal subduction inferred from numerical modelling. *Geophys. J. Int.* 166, 923–938. doi:10.1111/j.1365-246X.2006.03058.x

Mele, G. (2012). Mapping the Moho across the northern and central apennine chain and eastern sicily-the teleseismic receiver functions method. THE EARTH EXPANSION EVIDENCE–A Challenge for Geology, Geophysics and Astronomy.

Minelli, L., and Faccenna, C. (2010). Evolution of the Calabrian accretionary wedge (central Mediterranean): CALABRIAN ACCRETIONARY WEDGE. *Tectonics* 29, TC4004. doi:10.1029/2009TC002562

Menardi Noguera, A., and Rea, G. (2000). Deep structure of the campanian-lucanian arc (southern apennine, Italy). *Tectonophysics* 324 (4), 239–265. doi:10.1016/S0040-1951(00)00137-2

Monaco, C., and Tortorici, L. (2000). Active faulting in the Calabrian arc and eastern Sicily. *J. Geodyn.* 29, 407–424. doi:10.1016/S0264-3707(99)00052-6

Monaco, C., Tortorici, L., Nicolich, R., Cernobori, L., and Costa, M. (1996). From collisional to rifted basins: an example from the Southern Calabrian arc (Italy). *Tectonophysics* 266, 233–249. doi:10.1016/s0040-1951(96)00192-8

Neri, G., Marotta, A. M., Orecchio, B., Presti, D., Totaro, C., Barzaghi, R., et al. (2012). How lithospheric subduction changes along the Calabrian Arc in southern Italy: geophysical evidences. *Int. J. Earth Sci.* 101 (7), 1949–1969. doi:10.1007/s00531-012-0762-7

Neri, G., Orecchio, B., Totaro, C., Falcone, G., and Presti, D. (2009). Subduction beneath southern Italy close the ending: results from seismic tomography. *Seismol. Res. Lett.* 80 (1), 63–70. doi:10.1785/gssrl.80.1.63

Nicolich, R. (2001). *Deep seismic transects*. Anatomy of an orogen: the Apennines and adjacent Mediterranean basins, 47–52.

Nicolosi, I., Speranza, F., and Chiappini, M. (2006). Ultrafast oceanic spreading of the Marsili Basin, southern Tyrrhenian Sea: evidence from magnetic anomaly analysis. *Geology* 34, 717. doi:10.1130/g22555.1

Ogniben, L. (1973). Schema geologico della Calabria in base ai dati odierni. *Geol. Romana* 12, 243–585.

Ortolano, G., Cirrincione, R., and Pezzino, A. (2005). PT evolution of alpine metamorphism in the southern aspromonte massif (Calabria-Italy). Schweiz. *Mineral. Petrogr. Mitt* 85 (1), 31–56.

Ortolano, G., Cirrincione, R., Pezzino, A., Tripodi, V., and Zappala, L. (2015). Petro-structural geology of the Eastern Aspromonte Massif crystalline basement (southern Italy-Calabria): an example of interoperable geo-data management from thin section–to field scale. *J. Maps* 11 (1), 181–200. doi:10.1080/17445647.2014.948939

Patacca, E., and Scandone, P. (1989). "Post-Tortonian mountain building in the Apennines. The role of the passive sinking of a relic lithospheric slab," in The lithosphere in Italy. Advances in Earth Science Research". It. Nat. Comm. Int. Lith. Progr., Mid-term Conf, 5-6 May 1987. Editors A. Boriani, M. Bonafede, G. B. Piccardo, and G. B. Vai (Rome, 157–176. Atti Conv. Lincei.80

Pepe, F., Sulli, A., Bertotti, G., and Cella, F. (2010). Architecture and Neogene to recent evolution of the Western Calabrian continental margin: an upper plate perspective to the Ionian subduction system, Central Mediterranean. *Tectonics* 29. doi:10.1029/2009TC002599

Piana Agostinetti, N., and Amato, A. (2009). Moho depth andV_p/V_sratio in peninsular Italy from teleseismic receiver functions. *J. Geophys. Res. Solid Earth* 114 (B6), B06303. doi:10.1029/2008jb005899

Polonia, A., Melis, R., Galli, P., Colizza, E., Insinga, D. D., and Gasperini, L. (2023). Large earthquakes along slow converging plate margins: calabrian Arc paleoseismicity based on the submarine turbidite record. *Geosci. Front.* 14 (5), 101612. doi:10.1016/j.gsf.2023.101612

Polonia, A., Torelli, L., Artoni, A., Carlini, M., Faccenna, C., Ferranti, L., et al. (2016). The Ionian and Alfeo-Etna fault zones: new segments of an evolving plate boundary in the central Mediterranean Sea? *Tectonophysics* 675, 69–90. doi:10.1016/j.tecto.2016.03.016

Polonia, A., Torelli, L., Mussoni, P., Gasperini, L., Artoni, A., and Klaeschen, D. (2011). The Calabrian Arc subduction complex in the Ionian Sea: regional architecture, active deformation, and seismic hazard. *Tectonics* 30, TC5018. doi:10.1029/2010TC002821

Pontevivo, A., and Panza, G. F. (2006). The lithosphere-asthenosphere system in the Calabrian Arc and surrounding seas – southern Italy. *Pure Appl. Geophys.* 163, 1617–1659. doi:10.1007/s00024-006-0093-3

Rovida, A., Locati, M., Camassi, R., Lolli, B., Gasperini, P., and Antonucci, A. (2022). *Catalogo Parametrico dei Terremoti Italiani (CPTI15), versione 4.0*. Istituto Nazionale di Geofisica e Vulcanologia (INGV. doi:10.13127/CPTI/CPTI15.4

Scandone, P. (1979). Origin of the Tyrrhenian Sea and Calabrian Arc. *Boll. Soc. Geol. Ital.* 98, 27–34.

Scandone, P., Patacca, E., Radoicic, R., Ryan, W. B. F., Cita, M. B., Rawson, M., et al. (1981). Mesozoic and cenozoic rocks from Malta escarpment (central mediterranean). *AAPG Bull.* 65 (7), 1299–1319.

Scarascia, S., Lozej, A., and Cassinis, R. (1994). Crustal structures of the Ligurian, Tyrrhenian and Ionian seas and adjacent onshore areas interpreted from wide-angle seismic profiles. *Boll. Geof. Teor. Appl.* 36, 141–144.

Scarfì, L., Barberi, G., Barreca, G., Cannavò, F., Koulakov, I., and Patanè, D. (2018). Slab narrowing in the Central Mediterranean: the Calabro-Ionian subduction zone as imaged by high resolution seismic tomography. *Sci. Rep.* 8, 5178. doi:10.1038/s41598-018-23543-8

Scarfì, L., Langer, H., Messina, A., and Musumeci, C. (2021). Tectonic regimes inferred from clustering of focal mechanisms and their distribution in space: application to the Central Mediterranean Area. *J. Geophys. Res. Solid Earth* 126 (1), e2020JB020519. doi:10.1029/2020JB020519

Scrocca, D., Doglioni, C., Innocenti, F., Manetti, P., Mazzotti, A., Bertelli, L., et al. (2003). CROP Atlas: seismic reflection profiles of the Italian crust. *Mem. Descr. della Carta Geol. d'Italia* 62, 15–46.

Selvaggi, G., and Chiarabba, C. (1995). Seismicity and P-wave velocity image of the southern Tyrrhenian subduction zone. *Geophys. J. Int.* 121 (3), 818–826. doi:10.1111/j.1365-246x.1995.tb06441.x

Sengör, A. M. C. (1979). The North Anatolian transform fault: its age, offset and tectonic significance. *J. Geol. Soc.* 136 (3), 269–282. doi:10.1144/gsjgs.136.3.0269

Speranza, F., Minelli, L., Pignatelli, A., and Chiappini, M. (2012). The Ionian Sea: the oldest *in situ* ocean fragment of the world? *J. Geophys. Res.* 117, B12101. doi:10.1029/2012JB009475

Stampfli, G. M., Mosar, J., Marquer, D., Marchant, R., Baudin, T., and Borel, G. (1998). Subduction and obduction processes in the Swiss Alps. *Tectonophysics* 296, 159–204. doi:10.1016/s0040-1951(98)00142-5

Tassis, G. A., Grigoriadis, V. N., Tziavos, I. N., Tsokas, G. N., Papazachos, C. B., and Vasiljević, I. (2013). A new Bouguer gravity anomaly field for the Adriatic Sea and its application for the study of the crustal and upper mantle structure. *J. Geodyn.* 66, 38–52. doi:10.1016/j.jog.2012.12.006

Tiberti, M., Orlando, L., Bucci, D., Bernabini, M., and Parotto, M. (2005). Regional gravity anomaly map and crustal model of the Central–Southern Apennines (Italy). *J. Geodyn.* 40 (1), 73–91. doi:10.1016/j.jog.2005.07.014

Tugend, J., Chamot-Rooke, N., Arsenikos, S., Blanpied, C., and Frizon de Lamotte, D. (2019). Geology of the Ionian Basin and margins: a key to the East mediterranean geodynamics. *Tectonics* 38, 2668–2702. doi:10.1029/2018TC005472

Ventura, G. (2013). Chapter 2 kinematics of the aeolian volcanism (southern Tyrrhenian Sea) from geophysical and geological data. *Geol. Soc. Lond. Memoirs* 37 (1), 3–11. doi:10.1144/m37.2

Wortel, M. J. R., and Spakman, W. (2000). Subduction and slab detachment in the Mediterranean-Carpathian region. *Science* 290, 1910–1917. doi:10.1126/science.290.5498.1910